JOTCS A
Journal of the Turkish Chemical Society
Section: A
Chemistry
TURKISH CHEMICAL SOCIETY

Removal of Cesium from Aqueous Solution by Adsorption onto Sivas-Yildizeli (Türkiye) Vermiculite: Equilibrium, Kinetic and Thermodynamic Studies

Hilmi Arkut AKALIN[1], Ümran HİÇSÖNMEZ[2*], Hatice YILMAZ[3]

[1]Manisa Celal Bayar University, Graduate School of Natural and Applied Sciences, 45030, Muradiye/Manisa, Turkey.

[2]Manisa Celal Bayar University, Faculty of Arts and Science, Department of Chemistry, 45030, Muradiye/Manisa, Turkey.

[3]Dokuz Eylül University, Faculty of Engineering, Department of Mining Engineering, 35390, Tınaztepe/İzmir, Turkey.

Abstract: In this study, cesium adsorption performance of raw vermiculite obtained from Sivas-Yıldızeli region of Turkey was investigated using batch adsorption method. In order to obtain the optimum adsorption conditions; different adsorbent dosages, contact times, solution pH's, initial cesium concentrations and temperature ranges were investigated. The concentration of cesium in solution was determined by ICP-OES. Kinetic studies demonstrated that adsorption process was in accordance with pseudo-second order kinetic model and equilibrium isotherm modeling studies showed that the process was compatible with Langmuir, Freundlich and Temkin adsorption isotherm models, indicating that Cs adsorption process had both physical and chemical character. Negative Gibbs energy values obtained from thermodynamic studies revealed that the adsorption process was spontaneous and had a high feasibility. Additionally, the negative enthalpy value indicated that process was exothermic, suggesting that the adsorbed Cs^+ ions decreased with increasing reaction temperatures. Positive entropy value showed that disorderliness between solid-liquid phase increased during adsorption. Results clearly indicate that vermiculite mineral has a promising potential in removing Cs^+ ions from aqueous media which leads mineral may also be used in decomposing and efficiently removing radioactive cesium from contaminated waters.

Keywords: Cesium, vermiculite, adsorption, adsorption kinetic models, adsorption isotherms.

Submitted: May 31, 2017. **Accepted:** November 13, 2017.

Cite this: Akalın H, Hiçsönmez Ü, Yılmaz H. Removal of Cesium from Aqueous Solution by Adsorption onto Sivas-Yildizeli (Türkiye) Vermiculite: Equilibrium, Kinetic and Thermodynamic Studies. JOTCSA. 2018;5(1):85–116.

DOI: http://dx.doi.org/10.18596/jotcsa.317771.

***Corresponding author .E-mails:** umran.hicsonmez@cbu.edu.tr, arkutakalin@gmail.com, hatice.yilmaz@deu.edu.tr.

INTRODUCTION

In 2011, Fukushima Daiichi Nuclear power plant accident occurred and many radionuclides were released into the environment. They caused a great environmental disaster to living metabolisms including humans, animals, and plants nearby because of the contamination provided by these nuclides. Although zeolites were used to prevent the radioactive damage in the power plant facility and surrounding areas, it was not complete enough (1).

Remarkably, ^{137}Cs is one of the most important radionuclides among contaminants released into the environment with nuclear accidents and weapon tests, since it has a very long half-life (30 years) and strong radiation energy (2). Cesium is a crucial radioisotope which can easily move with aqueous media and has almost unlimited solubility in liquid systems, as well as incorporating into soil environment and aquatic organisms, harming them with an untolerated degree of γ and β radiation (3,4). In addition, radiocesium causes significant harm to human health, mostly triggering the incidence of thyroid cancer since it is strongly absorbed by the body via ingestion when exposed to cesium (5).

In order to prevent these negative effects, cesium must be removed from the environment efficiently and adsorption is the most effective method among many techniques used in removing cesium ions in aqueous media such as chemical precipitation, coagulation, membrane process, ion exchange column concerning its low cost, wide range of applicability and the possibility of various types of sorbent selection (6–10). Clay minerals are favorable for adsorption of radioactive components due to their environmental friendly character, abundance and ideal sorption features for specific kinds of metal ions (11).

Vermiculite is a typical 2:1 phyllosilicate clay mineral composed of alumina and magnesia formed between dual tetrahedral silicate sheet and the central chemical structure consists of magnesium octahedral structure (12,13). This mineral has a high surface area, layer charge density, and cation exchange capacity as well as it is reserved worldwide abundance, thus has ideal properties to be used as a powerful removal agent for monovalent cations such as cesium metal (14,15).

For the aim of removing radioactive cesium from radio-contaminated wastes using vermiculite, many studies were conducted since the 1960s, and the mineral was used as an efficient adsorbent for ^{137}Cs in nuclear reactor laboratory column (16–20). Additionally, the Japan Atomic Energy Agency research group (JAEA) investigated the adsorption behavior of radioactive cesium using vermiculite obtained in Fukushima Prefecture, and revealed that vermiculite has a significant potential in adsorbing large amounts of cesium ions due to the local rearrangement of mineral interlayer formation in relation to electrostatic interactions between positively charged cesium ions and oxygen atoms (21). Hence, as the amount of adsorbed cesium ions and the

other mobilized particles, which have similar chemical properties with cesium at one side of interlayer increases, interactions between the other sides of the interlayer is weakened and opposite clay interlayer is separated due to excess concentration of adsorbate ions. With this way, cesium ions at solution media could be gradually adsorbed with newly formed clay layer surface with strong ionic interactions and this sorption approach is called as domino toppling. Domino toppling effect of vermiculite was enlightened by a small angle X-ray scattering method where X-ray irradiates the sample, and the microscopic structure of the sample is determined by analyzing the intensity of the scattered X-ray as a function of the scattering angle.

Since vermiculite has excellent cesium adsorption properties summarized above, we have planned to use vermiculite mineral reserved in Sivas-Karakoç mine of Turkey for efficient removal of cesium ions in aqueous media. For this purpose, we investigated the effect of adsorbent dosage, contact time, pH, initial metal ion concentration, reaction temperature, equilibrium adsorption modeling, kinetic modeling and thermodynamic studies on cesium adsorption, which are important indicators for better understanding the sorption mechanism.

EXPERIMENTAL METHODS

Materials

Raw vermiculite was obtained from Organik Madencilik Corporation in Sivas-Yıldızeli region (Sivas-Karakoç mine). Stable ^{133}Cs as CsCl (Sigma-Aldrich), HNO_3 (Merck), HCl (Merck), NaOH (Merck), KCl (Sigma-Aldrich), oxalic acid (Sigma-Aldrich), ammonium acetate (Merck) and other chemicals used in the study were in analytical grade. Stable cesium chloride salt was used in the present study due to its radiochemical similarity with radioactive ^{137}Cs.

Apparatus

Hanna HI-221 pH meter, a GFL 1083 batch adsorption shaker, an AX224 Sartorius 220 g analytical scales, a Retsch RM-2OO automatic agate mortar, a Perkin Elmer Spectrum BX FT-IR spectrometer, a Rigaku Miniflex II XRD device, a Panalytical Axios XRF device, a Perkin Elmer Optima 8000 ICP-OES device were used in experiments.

Preparation of raw vermiculite sample

Vermiculite sample was ground to particle size to 355-400 μm with Retsch RM 200 mortar. In order to remove the water-soluble impurities from the sample, 10 g of raw vermiculite was dispersed in 250 mL distilled water and shaken in a batch shaker for 12 hours. After washing with distilled water, the sample was carefully removed from the glass tube and dried in an oven at 80^{o}C for 4 hours.

Characterization methods

Physicochemical analysis

Cation exchange capacity (CEC), bulk density and isoelectronic point of vermiculite were obtained with potentiometric technique, pycnometer, and pH difference methods, respectively.

XRD and XRF analysis

Quantitative chemical analysis of the sample was conducted with an XRF device (Panalytical Axios) in General Directorate of Mineral Research and Exploration Foundation, Analysis and Technology Laboratory, Ankara-Turkey. Mineralogical analysis of the sample was realized with XRD device, equipped with Cu X-ray tube, C monochromator and ICDD database (Rigaku Miniflex II) in Dokuz Eylül University Department of Mining Engineering. XRF analysis provided the quantitative amounts of chemical compounds exist in the mineral formation. XRD analysis enlightened and verified the crystal structure of vermiculite mineral.

Batch adsorption studies

Stock Cs^+ solution (1000 mg/L) was prepared by dissolving 0.1265 g of CsCl in 100 mL of distilled water. After preparation of the stock solution, approximately 3 mL of 0.5 N HNO_3 was added to media and the solution was shaken thoroughly. Solution pH values were arranged using 0.01/0.1 N of HNO_3 and NaOH. In order to find optimum Cs adsorption conditions; different amounts of adsorbent (0.05, 0.1 and 0.2 g), contact time (1, 2, 3, 4, 5, 6 and 8 hours), solution pH's (3, 4, 6, 7, 8, 9 and 10), initial Cs concentrations (100, 175, 200, 250, 300 mg/L) and reaction temperatures (25, 40, 50, 70°C) were studied and evaluated.

The specific amount of vermiculite mineral was weighed, and adsorption experiments were realized with appropriate CsCl solutions into 50 mL plastic test tubes. pH of the suspension was arranged to the desired level, noted as arrangement pH. The solution volume was rearranged to 25 mL by adding distilled water into the test tubes. The suspension was shaken for a suitable time in a batch shaker and then filtered using blue Whatman filter paper.

Liquid section was poured into the volumetric flask and prepared for ICP-OES analysis (Perkin Elmer Optima 8000). In order to calculate the amount of adsorbed Cs^+ ions on vermiculite layer, equation given below was used;

$$Q_e(mg/g) = \frac{(C_0 - C_e)V}{W} \qquad \textbf{(Eq. 1)}$$

Q_e = Amount of adsorbed Cs^+ ions on vermiculite layer (mg/g)

C_0 = Initial Cs^+ ion concentration (mg/L)

C_e = Equilibrium Cs^+ ion concentration (mg/L)

V = Volume of solution (L)

W = Amount of adsorbent (g)

Desorption studies

Since cesium is a radioactive isotope, it is crucial to regain Cs^+ ions back to solution media according to radioactive waste management laws in order to prevent negative effects caused by radio-contamination. Therefore, It is important to detect the desorption conditions where Cs^+ ions are recovered. For this purpose, different eluent solutions were used to regain cesium and observe the desorption conditions under different temperatures. In this respect, Cs^+ loaded vermiculite samples were mixed with 10 mL of 0.5 and 1 M of oxalic acid solutions in batch adsorption device under 25, 45 and 65°C for 2 h and recovered suspensions were filtered. Subsequently, aqueous phases were separated and the amount of desorbed Cs^+ ions were detected with ICP-OES analysis.

Similarly, Cs^+ loaded samples were contacted with 10 mL of ammonium acetate and HCl (0.5 and 1 M) solutions in batch adsorption device under 25 °C for 2 h, filtered and the filtrate was analyzed with ICP-OES. For regeneration of Cs in distilled water media, loaded mineral samples were mixed with 10 mL of distilled water in batch adsorption device under 25 °C for 2 h, then the Cs concentration in the bulk solution phase was determined by ICP-OES. Percentage of desorbed Cs^+ ions was calculated using equation given below;

$$\%\text{Desorption efficiency} = \frac{\text{Amount of } Cs^+ \text{ desorbed}}{\text{Amount of } Cs^+ \text{ adsorbed}} \text{x}100 \qquad \textbf{(Eq. 2)}$$

Potassium interference effect studies

IA group elements have similar features concerning their molecular orbital structures and electronic configuration. Natural soil samples include many cations such as Na^+, K^+, Mg^{2+}, and Ca^{2+}. Especially K^+ has an interesting effect of interfering the sorption of Cs^+ ions with different kinds of adsorbents regarding its ionic radius and chemical character (22).

Thus, to examine the effects of K^+ presence in Cs adsorption, 0.2 g of raw vermiculite sample was weighed and 5 mL of 1265 mg/L CsCl solution included 1000 mg/L Cs^+ ions poured into test tubes. At pH 8, the concentration of K^+ in solution varied from 100 and 400 mg/L, respectively. The volume of the solution was completed to 25 mL using distilled water and desorption experiments were realized at 25°C for 4 h. Resulting suspension was filtered, and the liquid was recovered for further determination of Cs concentration with ICP-OES.

RESULTS AND DISCUSSION

Physicochemical properties

Cation exchange capacity (CEC) of raw vermiculite was determined with a potentiometric technique using 0.5 N HCl (23) and calculated as 205 meq/100 g and this is a good value compared with other studies in the literature (24,25).

The bulk density of raw vermiculite samples containing 4% impurity was obtained as 0.909 g/cm^3 using pycnometer which is in good terms with the values reported by Organik Madencilik Mining Corporation where the samples were obtained (26).

The isoelectronic point of any adsorbent is crucial since it is an indicator of the point where maximum ionic adsorption takes place at specified pH point, and no uptake of adsorbate ions occur after that pH point, concerning ionic interactions. Hence, the isoelectronic point of raw vermiculite was obtained with given procedure (27): ΔpH value was calculated with the equation $\Delta pH = pH_{final} - pH_{initial}$ and the ΔpH (y-axis) vs. pH initial (x-axis) were plotted (not shown). The intercept point of the graph with x-axis was accepted as an isoelectronic point of vermiculite and was determined as pH 7.

Chemical and Mineralogical properties

Chemical components exist in mineral formation was enlightened using XRF technique and given in Table 1. For comparison, chemical analysis of another vermiculite sample obtained from the same region (Sivas-Yıldızeli, Karakoç mine) conducted by Üçgül and Addison (28,29) was investigated and the results demonstrated that SiO_2, TiO_2 and Na_2O contents of both minerals are similar.

Table 1: Chemical composition of raw vermiculite.

Element Oxides	Percentage (%w/w)
SiO_2	36.3
MgO	14.6
Al_2O_3	14.8
K_2O	4.8
Fe_2O_3	12.4
TiO_2	2.7
CaO	4.2
Na_2O	0.3
(LOI) Loss of Ignition	9.10

Mineralogical compositions of the raw sample determined by XRD were given in Figures 1 and 2. As shown in Figure 1, it was mainly composed of vermiculite, hydrobiotite, and cordierite while containing minor amounts of calcite, and trace amounts of sanidine.

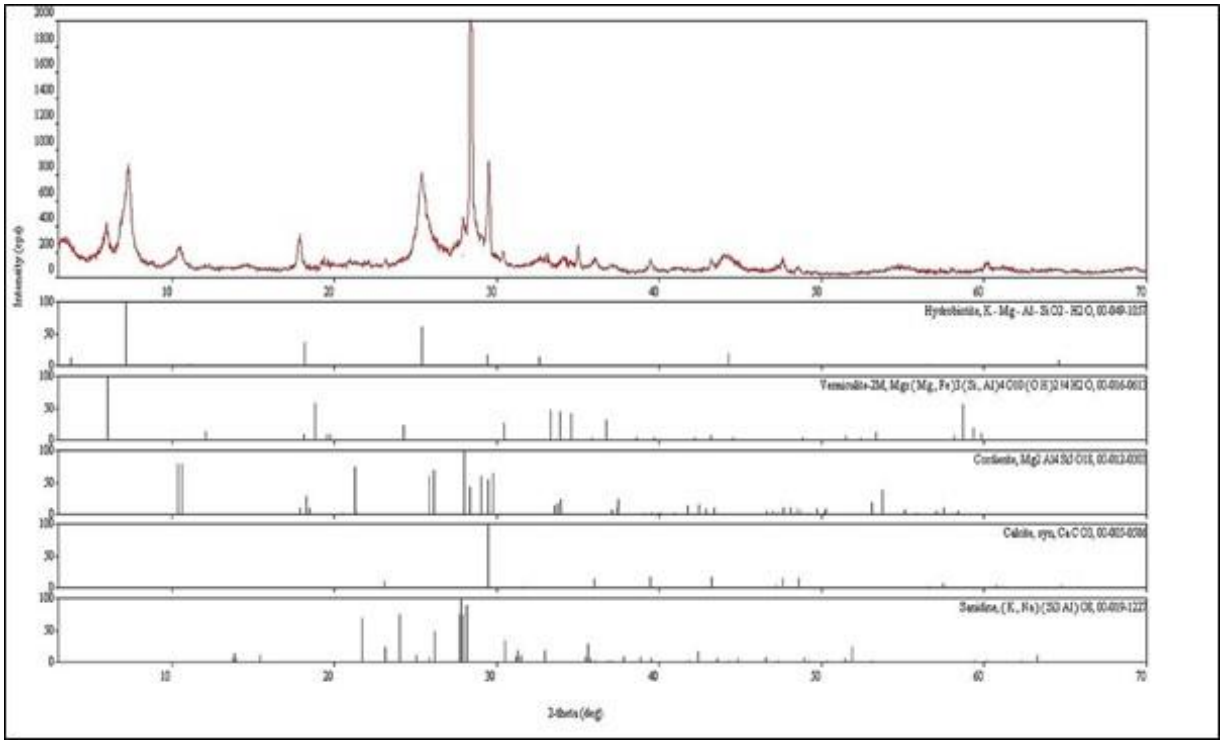

Figure 1: XRD diagram of Sivas-Yıldızeli vermiculite and other minerals in the formation.

The basal plane (100) of vermiculite and hydrobiotite mineral crystal structures are swollen when they collect water and organic molecules (such as ethylene glycol). When they are heated, however, the water and hydroxides are removed from their formation. Thus, changes occur in distances between the interlayers and the crystal structure. In order to reveal these changes, oriented samples were prepared by sedimentation. Samples were glycosylated and heated. The glycosylation procedure was materialized at 60 °C for 18 h under exposure to glycol vapor. Additionally, the heating procedure was carried out in oriented mineral samples under 550 °C for 1 h.

After these procedures, XRD diagrams were obtained, and the results were evaluated. According to the results, as seen in Figure 2, the peak corresponding to vermiculite in 15.33 Å was expanded to 18.28 Å. Peaks of other minerals were not affected by glycosylation. Thus, there were not any changes for their peaks. However, it was detected that peaks corresponding to vermiculite and hydrobiotite for the sample materialized under 550 °C for 1 h have been fully removed.

On the other hand, under these conditions two major enormous peaks were seen in 10.16 and 3.34 Å. The reason is, with the heating process; as H_2O and OH groups in the formation of

vermiculite and hydrobiotite were removed; the crystal structure of minerals was decomposed and transformed into an illite formation. Consequently, two characteristic peaks of illite (10.16 and 3.34 Å) were formed (Figure 2).

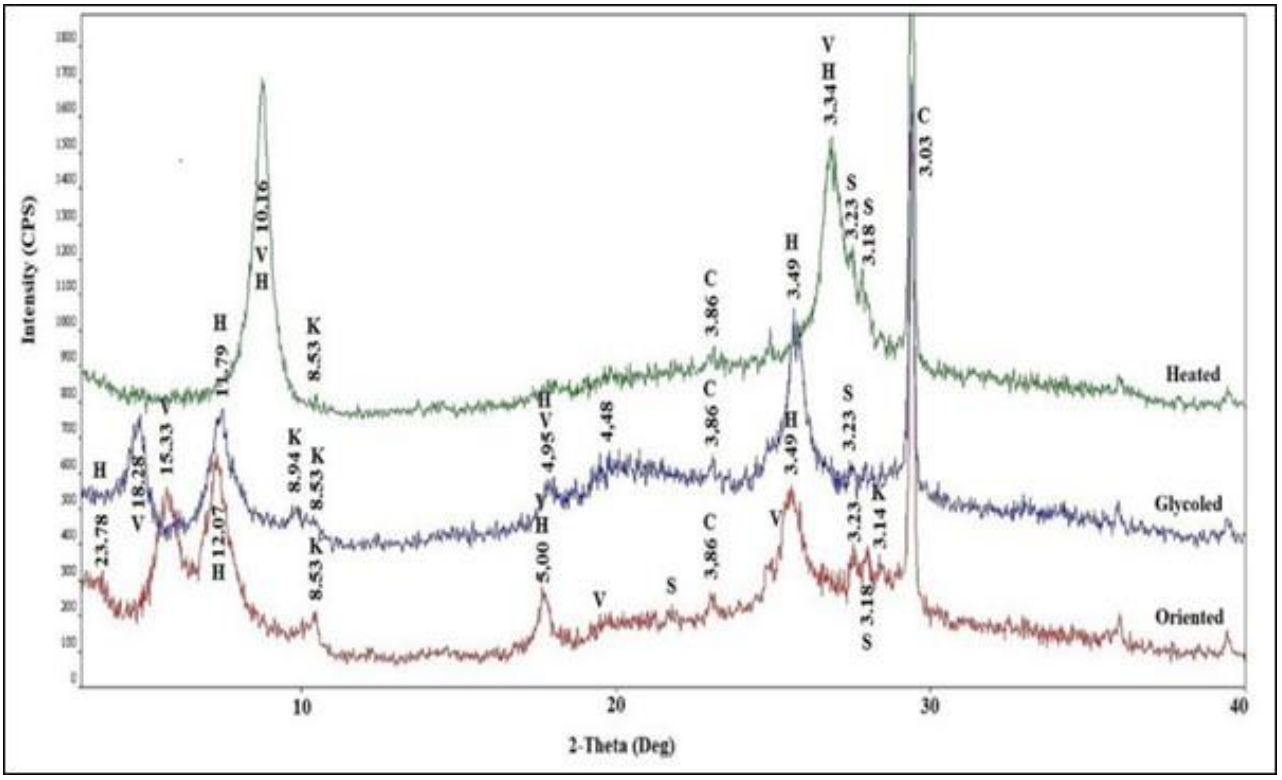

Figure 2: XRD peaks of Sivas-Yıldızeli vermiculite.

Cordierite, calcite, and sanidine minerals were affected neither by glycosylation procedure nor by the heating procedure under 550 °C. That is why these minerals are stable under these conditions. Thus, there were not any changes reported in their peaks. Therefore, peaks were unchanged after glycosylation and heating. As known, calcite is calcined at 1000 °C and decomposed as the reaction given below, but it is stable at 550 °C.

$$CaCO_3 \longrightarrow CaO + CO_2$$

In a study conducted by Ehsani (30), the crystal structure of a vermiculite sample obtained from South Africa was enlightened with XRD technique. Ehsani *et al.* investigated XRD peaks of the mineral by exposing it to heat and compared it with an untreated sample. They found that heated vermiculite showed characteristic peaks in 3.34 and 9.98 Å, thus compared with the current study; these peaks are identical with Sivas-Yıldızeli vermiculite, which illustrated 3.34 and 10.16 Å peaks.

As for unheated African vermiculite, peaks shown in 3.47, 4.91 and 11.82 Å are identical with Sivas-Yıldızeli vermiculite, which gave peaks in 3.49, 4.95 and 11.79, respectively. In another

study carried out by Yalçın *et al.* (31), they collected Sivas vermiculite for XRD analysis identification. Peaks found in 3.34 and 9.93 Å are nearly similar with that of peaks obtained in the current study (3.34 and 10.16 Å).

FT-IR analysis

Figure 3 illustrated FT-IR spectrum of Sivas-Yıldızeli vermiculite. As seen in the figure, the peak obtained in 3423 cm^{-1} with medium intensity, corresponded to stretching vibrations of OH and silanol groups, peak obtained in 1631 cm^{-1} with low intensity corresponded to bending vibrations of OH groups, major peak obtained in 1012 cm^{-1} with high intensity corresponded to stretching vibrations of Si-O and Al-O and finally, peak obtained in 466 cm^{-1} with high intensity corresponded to vibrations of Si-O-M (M: Si, Al, Mg, Fe) (30).

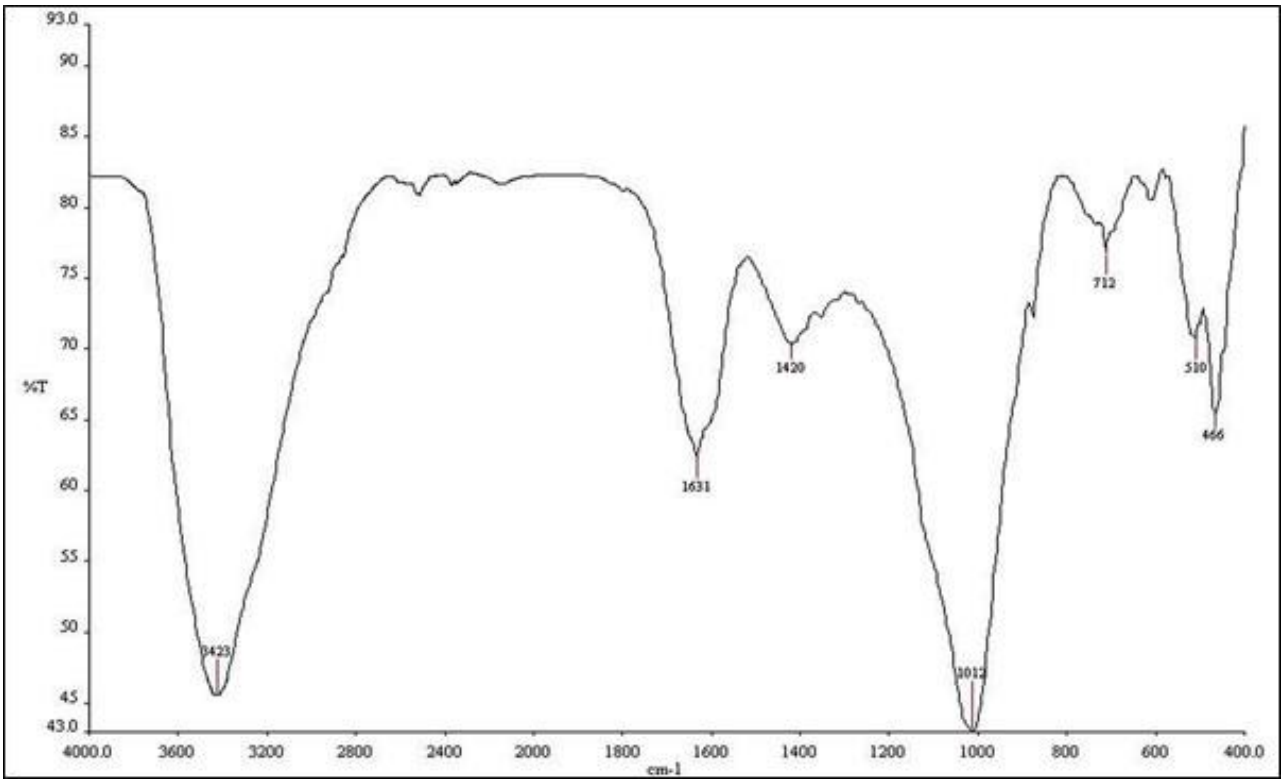

Figure 3: FT-IR spectrum of Sivas-Yıldızeli vermiculite.

Adsorption study

Effect of adsorbent dosage

0.05, 0.1 and 0.2 g of (2 g/L, 4 g/L, and 8 g/ L) raw vermiculite were used to find the optimum adsorbent dosage for cesium adsorption in 25 mL. Results demonstrated that adsorbed Cs^+ ions gradually increased with the increasing adsorbent dosage. Thus, the optimum adsorbent dosage for Cs adsorption process was obtained as 0.2 g of vermiculite. Hadadi *et al.* (4) proposed that Cs adsorption on natural vermiculite increased with increasing mineral dosage due to providing more active sites for adsorbing more Cs^+ ions in media, as seen in the current study. Kim *et al.* (2) reported that %Cs adsorption values increased with increasing sorbent concentrations.

However, adsorption capacities were decreased due to the increase of unsaturated sorption sites, which was in accordance with our results.

Figure 4 illustrates %Cs adsorption/Qe (mg/g) vs adsorbent dosage (g) plot, respectively. As seen in the figure, increasing the adsorbent dosage from 0.05 to 0.2 g caused a great difference in Cs uptake and the highest Cs sorption yield was obtained as 82.03% using 0.2 g of mineral.

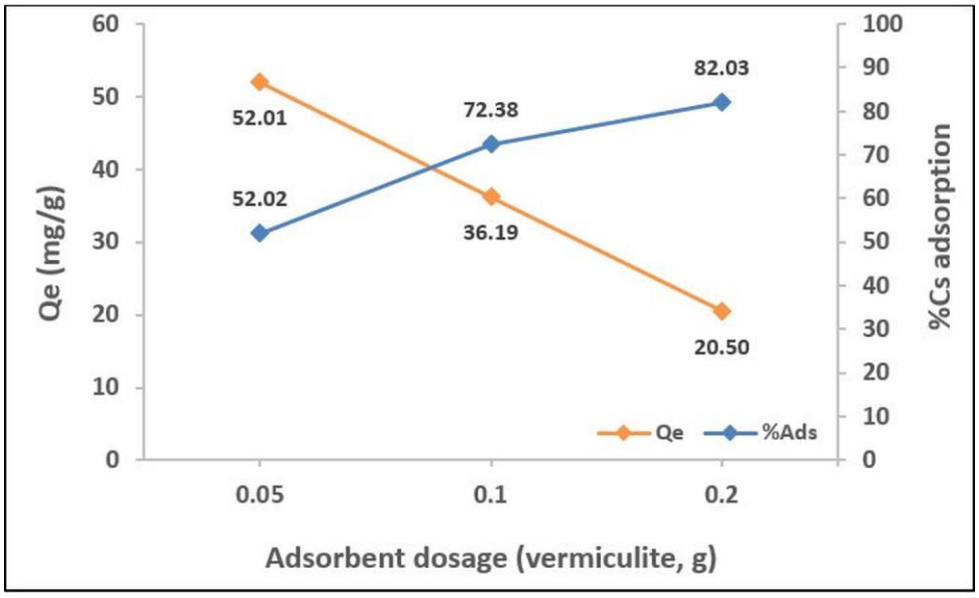

Figure 4: Effect of adsorbent dosage (Initial Cs concentration: 200 mg/L; Volume; 25 mL, Solution pH: 6; Contact time: 4 h; Reaction temp: 25°C).

Effect of contact time and reaction kinetics

In order to create kinetic modeling regarding the adsorption process, the effect of different contact times on Cs adsorption was investigated. A series of batch contact time experiments were performed to define and evaluate the optimum Cs ion sorption by the vermiculite, and the filtrate solution was checked by ICP-OES after each fraction. Experiments were conducted duplicate, and average %Cs adsorption/Qe values including standard deviations were included.

Results indicate, clearly, that Cs adsorption using vermiculite is not strongly depended on contact time since the equilibrium concentration of adsorbed Cs ions (Qe, mg/g) and adsorbed Cs ion percentage (Cs%) are very close in different time intervals (82% adsorbed Cs for 3 h, 82% for 4 h, 84% for 5 h) (Fig 5). Consequently, the optimum contact time was detected as 5 h.

In literature, similar behaviors have been previously reported about Cs^+ adsorption on different types of adsorbents (2,3). Khandaker *et al.* (32) studied the Cs sorption behavior of HNO_3 modified bamboo charcoal and the results demonstrated that Cs^+ ion uptake has not changed significantly with contact time, as was seen in the current study. Similarly, Yang *et al.* (33) found that Cs adsorption capacity of CuHF modified leather scrap stayed steady between 240 and 480 min (4–8 h), which showed a similar Cs sorption behavior with our study.

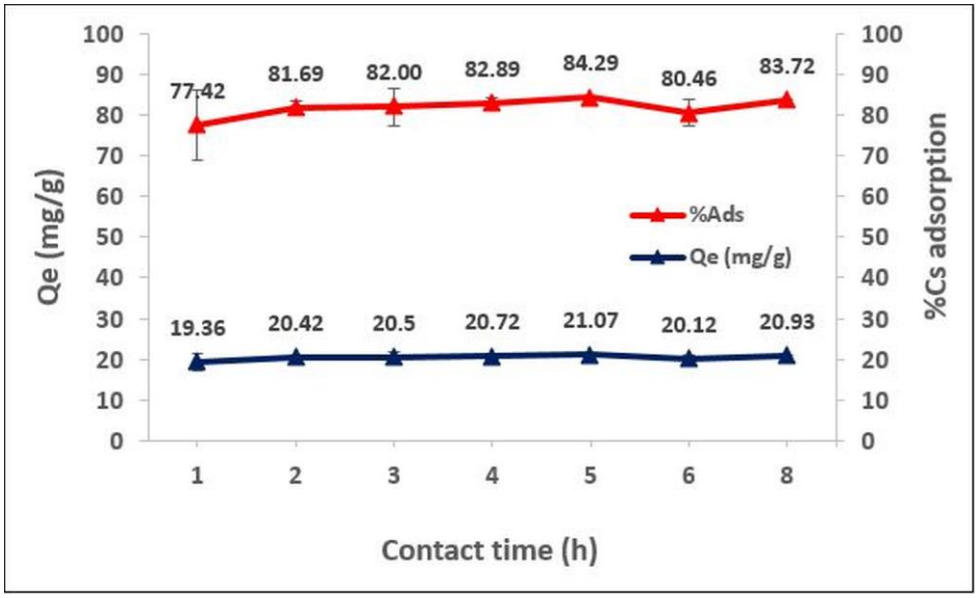

Figure 5: Effect of contact time (Adsorbent dosage: 0.2 g; Initial Cs concentration: 200 mg/L; Volume; 25 mL, Solution pH: 6; Reaction temp: 25°C).

Pseudo-First Order kinetic model (Lagergren model)

This model was found by Lagergren in 1898 and has been applied to many studies since (34). Mathematical expression of Lagergren model is given by Equation 3, where Q_e: Amount of Cs ions adsorbed at equilibrium (mg/g), Q_t: Amount of Cs ions adsorbed at equilibrium at a specific time interval (mg/g), k_1: Lagergren rate constant (1/h), t: Contact time (h). Results of kinetic modeling study are illustrated below, which is built by kinetic parameters, respectively.

$$\log(q_e - q_t) = \log(q_e) - \frac{k_1}{2.303} t \qquad \textbf{(Eq. 3)}$$

Pseudo-first order kinetic rate constant (k_1) was determined as 0.1089 h^{-1} and R^2 value of pseudo-first order kinetic model was found as 0.386, indicating that Cs-vermiculite adsorption process is not suitable with Lagergren kinetic model (graphic not shown). Theoretical (1.89 mg/g) and experimental Qe (21.75 mg/g) values proved this issue, as they are not even close.

Pseudo-Second Order kinetic model (Ho model)

Ho and McKay found pseudo-second Order kinetic model in 1999, and this model has a wide variety of applications to various adsorption systems (35). Mathematical expression of Ho model is given in Equation 4, where Q_e: Amount of Cs ions adsorbed at equilibrium (mg/g), Q_t: Amount of Cs ions adsorbed at equilibrium at a specific time interval (mg/g), k_2: Ho rate constant (g/mg.h), t: Contact time (h). Fig 6 represents pseudo-second order kinetic model given for Cs-vermiculite adsorption process, parameters of Ho model applied to the current study is given above.

$$\frac{t}{q_t} = \frac{1}{K_2 q_e^2} + \frac{t}{q_e} \qquad \textbf{(Eq. 4)}$$

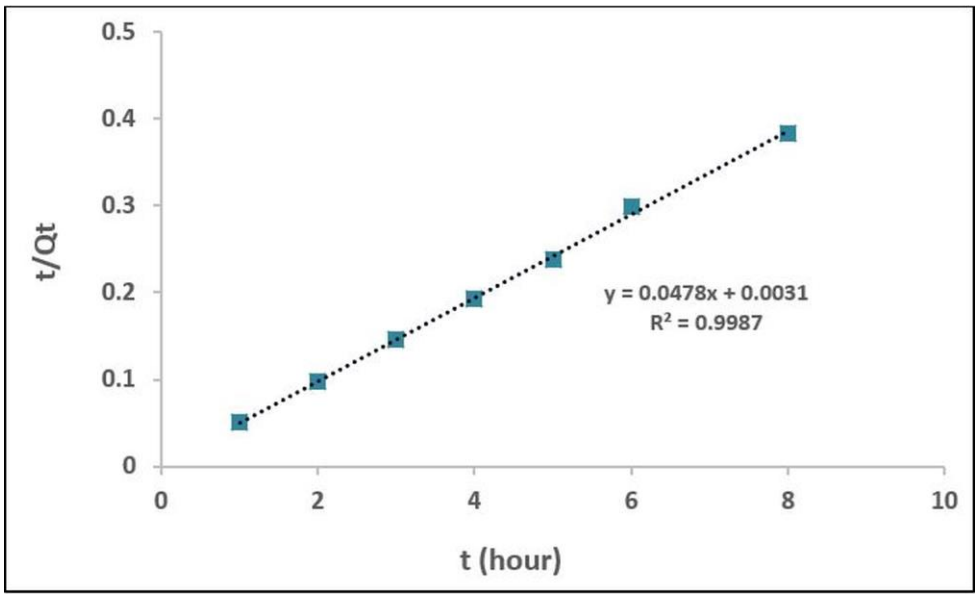

Figure 6: Pseudo-Second order Ho kinetic model plot of the Cs-vermiculite adsorption process.

Pseudo-second order kinetic model rate constant (k_2) was obtained as 0.7371 g/mg.h. More importantly, high regression value found as 0.9987 and close experimental (21.75 mg/g) and theoretical (20.92 mg/g) Qe values suggested that Cs-vermiculite adsorption operation was in accordance with pseudo-second order kinetic model.

Elovich kinetic model

This chemisorption model was established by Zeldowitsch in 1934 (36) and applied to describe the rate of adsorption of carbon monoxide on manganese dioxide that decreased exponentially with an increase in the amount of gas adsorbed (37). Mathematical linear expression of Elovich equation is given in Equation 5 (38), where Q_t: Amount of Cs ions adsorbed at equilibrium at a specific time interval (mg/g), α and β: Elovich rate constants, t: Contact time (h). Linear regression value of Elovich Kinetic model was obtained as 0.5695 suggesting that Cs-vermiculite adsorption was not compatible with this model (graphic not shown).

$$q_t = a + b\ln t \qquad \textbf{(Eq. 5)}$$

Weber-Morris kinetic model (Intraparticle model)

Adsorption of cesium ions on vermiculite pores is depended upon three stage consecutive stage process; boundary layer diffusion (film diffusion), intraparticle diffusion and adsorption on the porous surface. Briefly, adsorbate molecules (Cs^+ ions) soluted in liquid media are mass transferred across the external film layer, which covered the outer section of adsorbent (vermiculite).

After Cs^+ ions are transferred across this film, they are moved into the inner sections of vermiculite pores, and this is known as intraparticle diffusion. When adsorbate molecules reach the active adsorption sites of the mineral, they are physically adsorbed onto porous layers.
In order to enlighten the type of diffusion kinetics mechanism concerning Cs adsorption onto vermiculite, Weber-Morris kinetic model (intraparticle model) was applied to present data by plotting q_t values against $t^{1/2}$ data.

Weber-Morris kinetic model expression is given in Eq. 6, where q_t: Amount of Cs^+ ions adsorbed in a given moment at equilibrium, K_{ipd}: Intraparticle diffusion rate constant, $t^{1/2}$: Root of adsorption contact time, C: Intercept defining the thickness of boundary layer in intraparticle diffusion mechanism. High C values correspond to thicker boundary layer (film layer) covering the external site of an adsorbent molecule (39).

$$q_t = K_{ipd} t^{1/2} + C \qquad \textbf{(Eq. 6)}$$

Intraparticle diffusion model parameters and the characteristics of diffusion kinetics regarding the adsorption of Cs on vermiculite pores are summarized below. For 1, 2, 3, 4, 5, 6, and 8 hours of adsorption, $t_{1/2}$ values were obtained as 1, 1.4142, 1.7320, 2, 2.2361, 2.4495, and 2.8284, respectively.

In the case of intraparticle diffusion is completely affecting the adsorption process, the plot q_t versus $t_{1/2}$ passes through the origin (40), which is not a valid situation in the current experiment as seen in Figure 7.

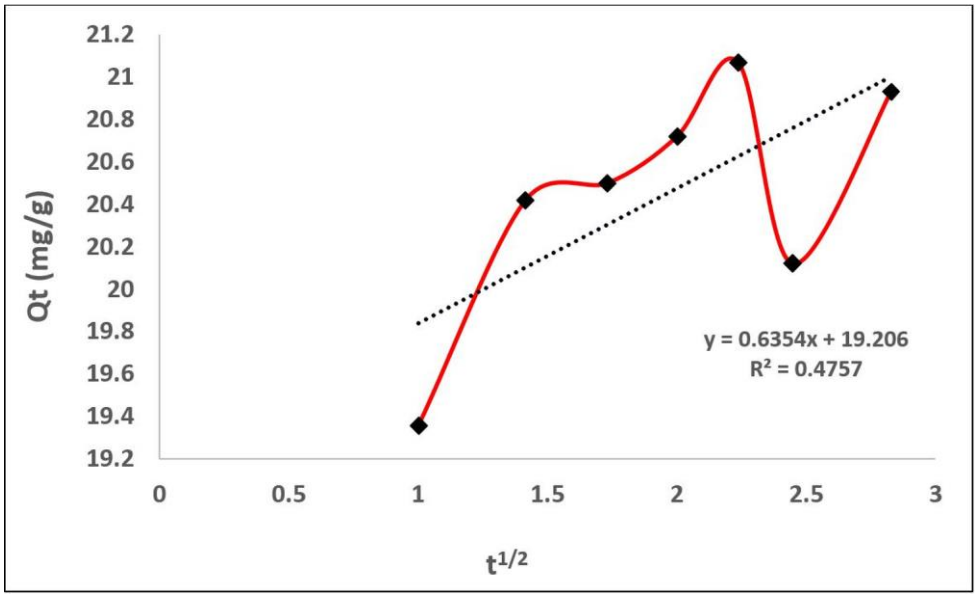

Figure 7: Weber-Morris kinetic model plot of Cs-vermiculite adsorption process.

That means that Cs adsorption on vermiculite layer consists of two-stage processes, the first part is rapid boundary layer diffusion and the second part is slower intraparticle diffusion. Consequently, Cs adsorption process onto vermiculite was not compatible with Weber-Morris kinetic model, since R^2 value of 0.4757 was quite low and unsatisfactory for the intraparticle process.

Effect of solution pH

In order to investigate the effect of pH on Cs adsorption, different solution pH's were studied and evaluated. Solution pH was rearranged to 3, 4, 6, 7, 8, 9 and 10 using appropriate acid/base solutions and pH meter, respectively. As shown in Figure 8, the percentage of adsorbed Cs^+ ions and amount of adsorbed Cs^+ ions at equilibrium were increased with increasing pH values until pH 9.2.

The reason is due to the negative electrostatic interactions covered the layer of vermiculite causing a more powerful affinity between positive charged Cs ions and mineral layer, thus increasing the amount of Cs^+ ions onto mineral (4). Additionally, high alkaline pH values caused the formation of cesium hydroxide complexes as negatively charged $Cs(OH_2)^-$ via hydrolysis, resulting in electrostatic repulsions with mineral layer surface and triggered the decrease in the amount of adsorbed Cs^+ (41,42).

Ding *et al.* (43) reported that Cs^+ uptake on the clay sample significantly decreased under pH 5 due to the competition between H_3O^+ and Cs^+ ions in acidic media. However, in more alkaline values, Cs^+ uptake was increased concerning the lower competition between H_3O^+ and Cs^+, more importantly, deprotonation of silanol and aluminol groups, providing a stronger affinity between active sites and cesium (3).

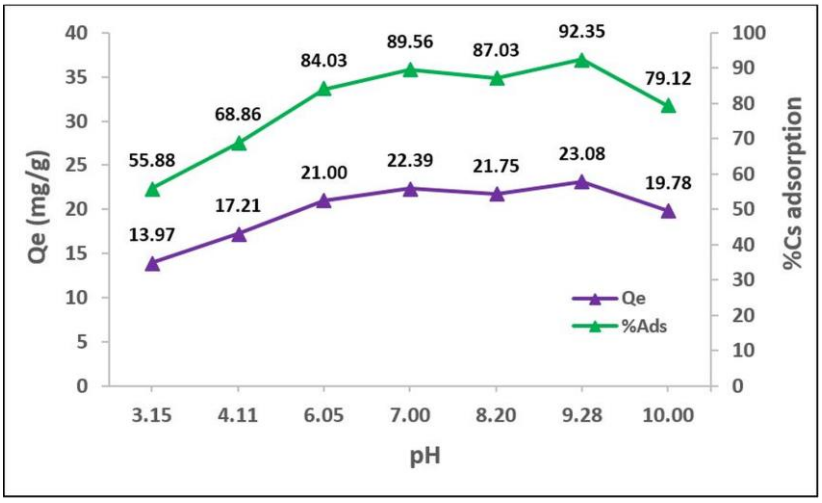

Figure 8: Effect of solution pH (Adsorbent dosage: 0.2 g; Initial Cs concentration: 200 mg/L; Volume; 25 mL, Contact time: 5 h; Reaction temp: 25°C).

Effect of initial Cs concentration and equilibrium isotherm modeling

Different concentrations of adsorbate and the effects of adsorption were investigated. Fig 9 demonstrates the effect of initial adsorbate concentration on Cs^+ adsorption process. Increasing adsorbate concentrations caused an increase in the amount of Cs^+ ions adsorbed onto the surface of the mineral, per 1 mg of Cs ion adsorbed in per 1 g of mineral, meaning mg/g. Even the adsorption percentage was found as 99% in 100 mg/L Cs concentration; it was decided to study with 200 mg/L Cs concentration for adsorption experiments.

Seaton *et al.* (44) observed that adsorption capacity of Cs (mg/g) using silica gel embedded phosphotungstic acid gradually increased with increasing Cs initial concentrations. Ding *et al.* (43) found that Cs^+ adsorption amount has increased proportionally with augmenting initial Cs concentrations. These results support gradual sorption increase behavior of Cs^+ with enhancing initial concentrations in our study.

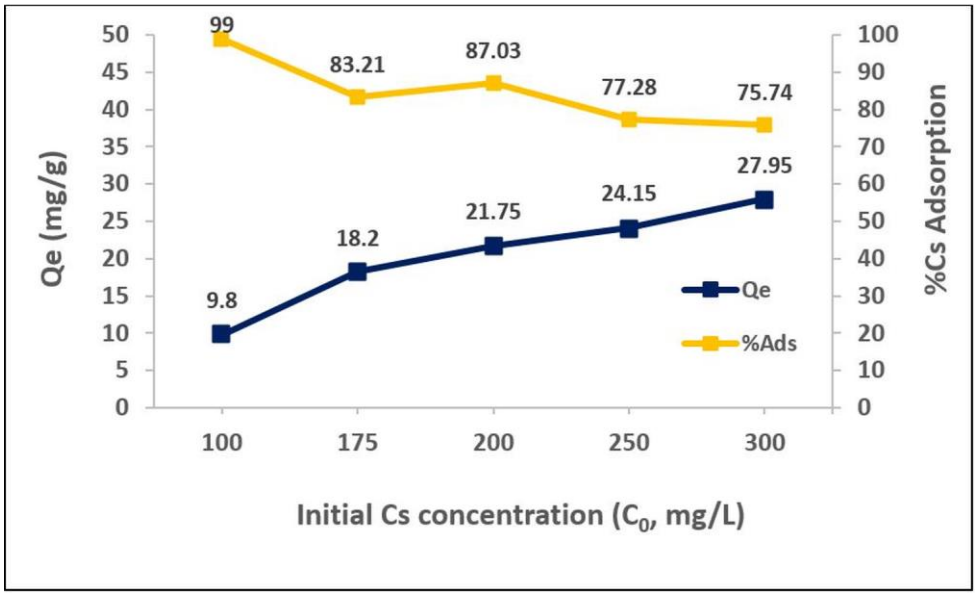

Figure 9: Effect of initial Cs concentration (Adsorbent dosage: 0.2 g; Solution pH: 8; Contact time: 5 h; Reaction temp: 25°C).

There are various kinds of adsorption isotherms used in the literature and the most important ones are reported as Langmuir (45), Freundlich (46), D-R (47) and Temkin (48) isotherms. Adsorption isotherms provide the knowledge and relation between the concentration of adsorbate ions in bulk solution and adsorbed amount of them at equilibrium, thus enlightening the efficiency and characteristics of the adsorption process. Present data were exposed to Langmuir, Freundlich, D-R, and Temkin isotherm models for further investigation of adsorption characteristics.

Langmuir isotherm model

Irving Langmuir established the Langmuir adsorption isotherm model in 1918 and described the gas-solid phase adsorption on activated carbon using this model (45). The general assumption of Langmuir adsorption isotherm model is that the adsorption takes place in a monolayer section of adsorbent and adsorption energies of adsorbate molecules are identically uniform. Thus, there are not any interactions between adsorbed metal ions on the porous surface of sorbent. Additionally, the processes that are compatible with Langmuir isotherm model are usually characterized by chemical adsorption, meaning after being reached to adsorption saturation point, which is called as maximum monolayer capacity, no following sorptions occur. This model was applied to many studies concerning the adsorption of various metal ions on different kinds of clay minerals for years (49–53).

Langmuir model is expressed in Equation 7, where Ce: Concentration of adsorbate ions in bulk solution at equilibrium (mg/L), Qe: Amount of adsorbed ions on adsorbent surface at equilibrium (mg/g), Q_{max}: monolayer saturation capacity (maximum monolayer capacity, mg/g), b: Langmuir constant related to adsorption energy (L/mg). Plotting Ce/Qe against Ce gives the slope of $1/Q_{max}$ and the intercept of $1/bQ_{max}$. Parameters of Langmuir isotherm and adsorption isotherm plot are demonstrated in Fig 10.

$$\frac{C_e}{q_e} = \frac{1}{bQ_{max}} + \frac{C_e}{Q_{max}} \qquad \textbf{(Eq. 7)}$$

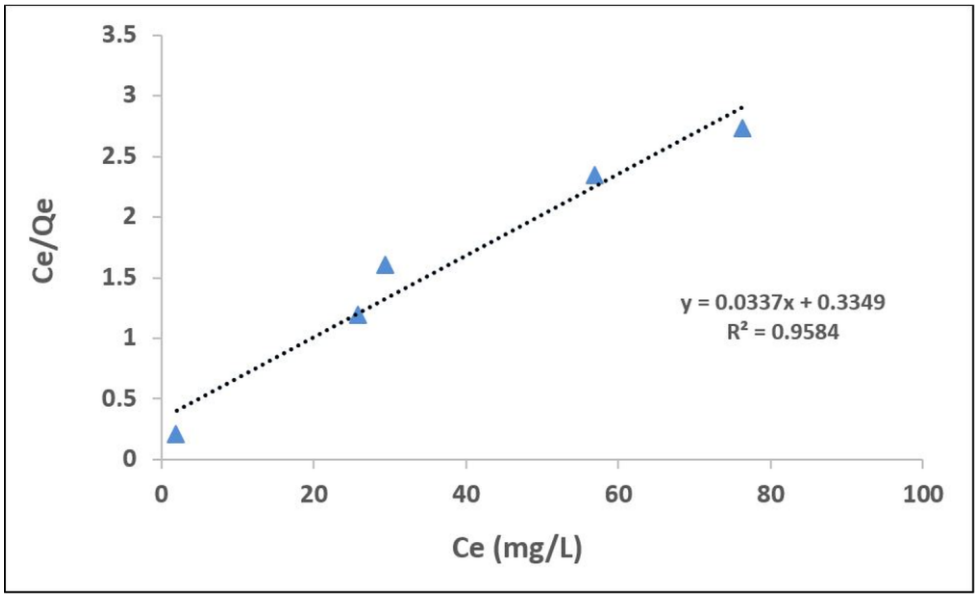

Figure 10: Langmuir adsorption isotherm plot for Cs adsorption onto vermiculite.

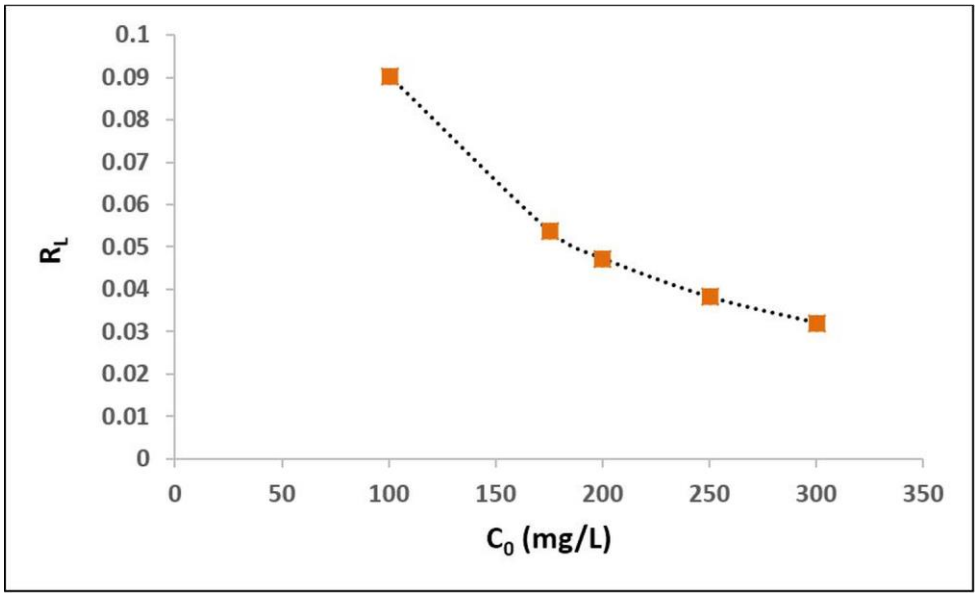

Figure 11: Variation of separation factor as a function of initial Cs concentration.

Applicability of Langmuir adsorption isotherm is verified by a dimensionless physicochemical constant given as separation factor, R_L. It defines either adsorption nature is favorable or not, thus it is an indicator of sorption feasibility. If R_L value >1: it indicates that the adsorption process is unfavorable, if R_L value is $0 < R_L < 1$: it is favorable, if $R_L = 0$: process is irreversible and finally if $R_L = 1$, it is linear (54). Separation factor (R_L) is mathematically illustrated in Equation 8, where R_L: separation factor, K_L: Langmuir constant (L/mg), C_0: Initial adsorbate concentration (mg/L). The connection between separation factor R_L and initial Cs concentration (between 100 and 300 mg/L Cs) is given in Fig 11.

$$R_L = \frac{1}{1 + K_L C_0} \qquad \textbf{(Eq. 8)}$$

Cesium adsorption process onto vermiculite surface was compatible with Langmuir isotherm model since linear regression value of Langmuir plot was obtained as 0.9584. Separation factor (R_L) values were found as 0.0904, 0.0538, 0.0473, 0.0382, and 0.0321, respectively (for 100-300 mg/L initial Cs). In addition, Langmuir constant related to the adsorption energy b was calculated as 0.1006 L/mg. Maximum adsorption capacity Q_{max} was determined as 29.67 mg/g.

These results indicate that Cs^+ ions were adsorbed on a monolayer section of porous vermiculite structure with uniform energies. R_L value being obtained lower than 1 proposed that adsorption of Cs onto the mineral was a favorable process and as seen in Fig 11, increasing initial metal concentrations caused R_L values to gained closer to zero value, meaning higher adsorbate concentrations were more appropriate for favorable Cs adsorption.

Freundlich isotherm model

This isotherm model was originally found by Freundlich in 1906 (46) and is based on a contrary idea with Langmuir's isotherm characteristics that the adsorption takes place on a heterogeneous porous surface of adsorbent and adsorption energies (enthalpy) of adsorbate molecules are not identical, referring that sorption enthalpy is dependent on the amount of adsorbate. Also, this model approves that the adsorption enthalpy decreases logarithmically with the increase of adsorbate fractions. Consequently, if an adsorption model is fitted with Freundlich model, it strongly suggests that a physical adsorption process is in effect with lower sorption energy than that of chemisorption (55,56).

Linear form of Freundlich adsorption isotherm model is mathematically expressed in Equation 9 where q_e: Amount of adsorbed ions at equilibrium (mg/g), K_f: Freundlich constant corresponding to approximate indicator of adsorption capacity (mg/g), 1/n: Adsorption intensity indicating that whether adsorption process is favorable or not, C_e: Concentration of metal ions in bulk solution at equilibrium (mg/L). Plotting $\log q_e$ against $\log C_e$ gives the slope of 1/n and the intercept of $\log K_f$, as it is demonstrated in Fig 12.

$$\log q_e = \log K_f + \frac{1}{n}\log C_e \qquad \textbf{(Eq. 9)}$$

1/n value is an important indicator for evaluating whether sorption is favorable or not since, if 1/n = 1, it corresponds that adsorption is linear, 1/n < 1 suggest that adsorption is a physical sorption and fits Freundlich model and finally if 1/n > 1, it means that adsorption is a chemical process. 1/n value also corresponds to the degree of adsorption heterogeneity, meaning the smaller 1/n values express higher heterogeneity (54).

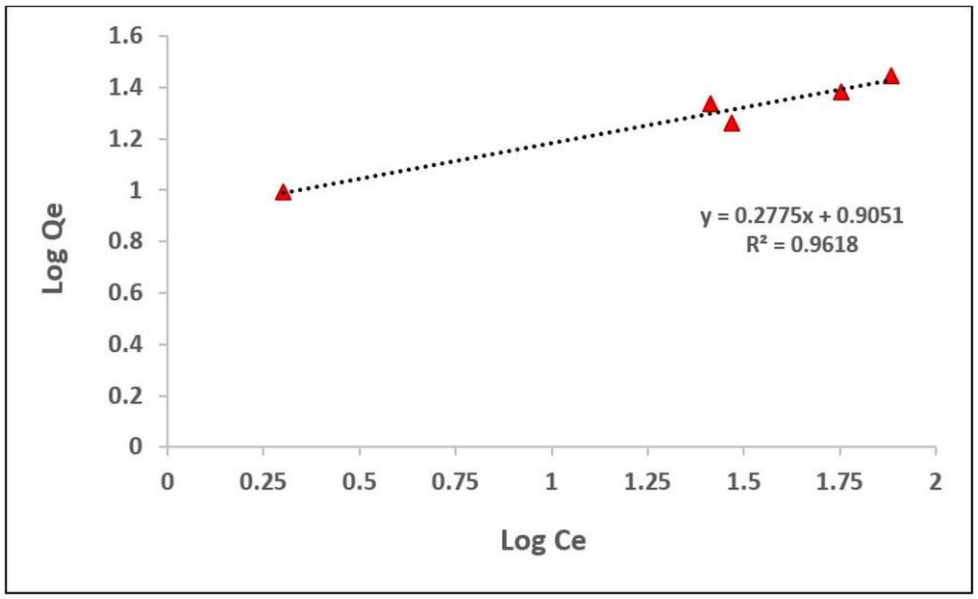

Figure 12: Freundlich adsorption isotherm plot for Cs adsorption onto vermiculite.

As displayed in Fig 11, high linear regression value of 0.9618 and excellent 1/n value being calculated lower than unity (n=3.6036, 1/n=0.2775) clearly explains that Cs adsorption onto the porous surface of vermiculite mineral is in accordance with Freundlich adsorption isotherm model and it is an indicator of the presence of a physical sorption. Thereby, these data provide that a physisorption process administrates sorption uptake of positively charged Cs ions onto the vermiculite mineral with a maximum adsorption capacity of 8.037 L/g.

Temkin isotherm model

Mikhail Temkin developed this model with a study based on the adsorption of hydrogen gas onto platinum electrodes in acidic solutions in 1940, thus is a modified Langmuir isotherm model (48). On the contrary with Freundlich isotherm model assumption, the model is based on the idea that the adsorption enthalpy decreases not exponentially, but linearly with the increase of adsorbate fractions and the binding energies of adsorbate molecules on the adsorbent surface is uniformly distributed because of the indirect adsorbate/adsorbent interactions (57). Linear form of Temkin isotherm model is displayed in Equation 10, where q_e: Amount of adsorbed ions at equilibrium (mg/g), C_e: Concentration of metal ions in the bulk solution at equilibrium (mg/L), B: Heat of adsorption constant (j/mol), B = RT/b where b: Temkin isotherm constant referring the heat of adsorption, A: Equilibrium binding constant (L/g), R: Ideal gas constant (8.314 j/mol.K), T: Absolute temperature (°K).

$$q_e = B\ln C_e + B\ln A \qquad \textbf{(Eq. 10)}$$

Figure 13 demonstrates the parameters of Temkin isotherm and plot of q_e versus ln C_e where the slope of the graphic is B and the intercept is B lnA. Temkin isotherm constant b derived from B constant refers to the heat of adsorption and is used to determine the adsorption characteristics, meaning whether the adsorption is a physical or chemical process (58). Empirical results demonstrated that adsorption of Cesium ions onto vermiculite surface showed a physical sorption character since Temkin isotherm constant b was found to be 541.46 j/mol, lower than 8 kJ/mol and this is supported by the results of Freundlich isotherm modeling. In addition, good linear regression value of 0.9139 indicates that adsorption process is fitted with Temkin isotherm model.

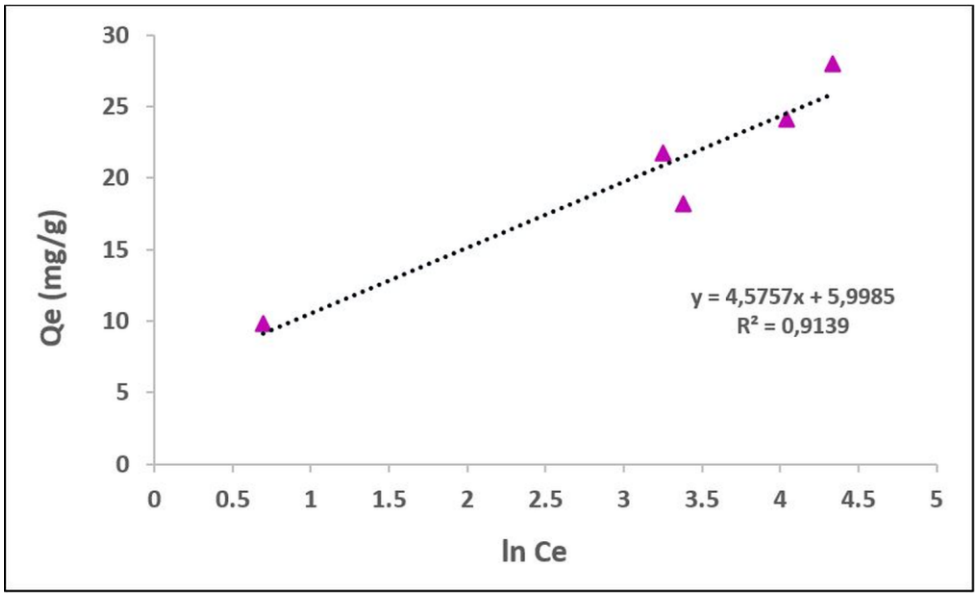

Figure 13: Temkin adsorption isotherm plot for Cs adsorption onto vermiculite.

Dubinin-Radushkevich (D-R) isotherm model

Dubinin-Radushkevich adsorption isotherm model (47) was developed in 1947 to describe the sorption of vapors onto microporous solids in order to express the adsorption mechanism with a Gaussian energy distribution on a heterogeneous surface. This model assumes that adsorption process follows a pore-filling mechanism and has been used to distinguish the physical and chemical adsorption using isotherm parameters concerning the sorption energy (59). Additionally, this model accepts that the adsorption curve is related to the porosity of adsorbent and often fit well with the high amount of solute activities with mid-range of concentrations. Linear expression of D-R isotherm model is demonstrated in Equation 11, where q_e: Amount of adsorbate ions adsorbed at equilibrium (mg/g), $K_{DR:}$ D-R isotherm constant (mol^2/kj^2) associated with mean free adsorption energy of adsorbate molecules per mole as they are transferred from solution media onto the adsorbent surface (60). Q_{max}: Theoretical isotherm saturation capacity (mg/g), ϵ: Polanyi potential (j/mol). Expression of Polanyi potential is also given in Equation 12. The D-R plot of $\ln q_e$ versus ϵ^2 gives the slope of isotherm constant K_{DR} and the intercept of maximum adsorption capacity, $\ln q_{max}$ as it is displayed in Fig 14.

$$\ln q_e = K_{DR}e^2 + \ln q_{max} \qquad \textbf{(Eq. 11)}$$

$$e = RT\ln(1 + \frac{1}{C_e}) \qquad \textbf{(Eq. 12)}$$

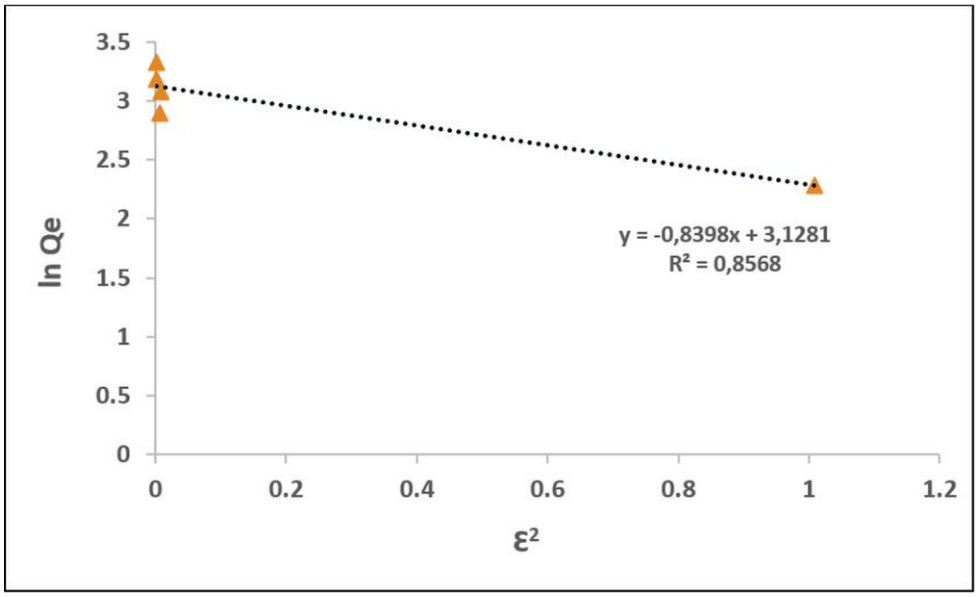

Figure 14: Dubinin-Radushkevich adsorption isotherm plot for Cs^+ adsorption onto vermiculite.

D-R adsorption isotherm constant; K_{DR} was found as 0.8398 mol^2/kj^2 and Q_{max} value corresponding to the maximum adsorption capacity of adsorbent, derived from Equations 11 and 12, was obtained as 22.38 mg/g.

One of the unique characteristics of D-R isotherm model is that it provides the type of sorption process using adsorption energy parameter given as E. According to present model, with the calculation of E; if E < 8 kJ/mol, that refers the adsorption is a physical process (physisorption) with Van der Waals interactions. if 8 < E < 16 kJ/mol, it indicates that adsorption of metal ions on adsorbent is a chemical process with higher sorption enthalpy, more likely with the domination of covalent bond interactions (61). The formula of adsorption energy E is shown in Equation 13.

$$E = \left[\frac{1}{\sqrt{2K_{DR}}}\right] \quad \textbf{(Eq. 13)}$$

As demonstrated in Fig 13, D-R isotherm plot is constructed with a temperature-dependent modeling, since ε and ε^2 values calculated for different temperatures affect the sorption curve, and the data fitted with model lied on the same curve. Adsorption energy is found as 0.772 kJ/mol, which is lower than the value of 8 kJ/mol, indicates that the adsorption of Cs^+ ions onto vermiculite surface is a physisorption process. In addition, linear regression value of 0.8568 is an unsatisfactory R^2 value, referring that sorption of Cs onto the porous structure of vermiculite mineral is not compatible with D-R isotherm model.

Effect of temperature and adsorption thermodynamics

Thermodynamic parameters are essential for the interpretation of the nature and characteristics of adsorption process concerning their physicochemical attributes. Gibbs free energy, adsorption enthalpy, and entropy hold fundamental knowledge about the character of sorption. Gibbs free energy change (ΔG^0), provides the information of whether the sorption process is spontaneous or not, meaning if it is necessary to give an external energy to the system in order to start the adsorption. Adsorption free enthalpy (ΔH^0) change gives the knowledge of the thermal character of the sorption, providing whether the sorption of metal ions on adsorbent is endothermic or exothermic and finally, adsorption free entropy change (ΔS^0) is an indicator of magnitude concerning the disorder among the adsorbate molecules and adsorbent.

If $\Delta G^0 < 0$ (negative): it indicates that the sorption occurs spontaneously without the need for an external energy. If $\Delta G^0 > 0$ (positive), it means the sorption does not take place spontaneously and the reaction mechanism needs a supportive force, mostly the heat energy. Usually, it is favorable for ΔG^0 to be spontaneous (negative value) for ideal sorption mechanism. Physicochemical expression of Gibbs free energy change (ΔG^0) and the equilibrium constant K_c are illustrated between Equation 14 and 17, respectively. R: ideal gas constant (8.314 j/mol.K) and T: absolute temperature (K).

Equilibrium constant (K_c) refers the ability of an adsorbent molecule to hold adsorbate ions onto its porous structure and amplitude of adsorbate mobility in the sorption media, regarding the ratio of adsorbed metal ions at equilibrium and concentration of metal ions in bulk solution (62). The general expression of ΔG^0 is given in Eq. 14 and rearranging ΔG^0 as $-RT\ln K_c$ from Eq. 15 gives the Eq. 17. The plot of $\ln K_c$ versus 1/T gives the slope of $\Delta H^0/RT$ and the intercept of $\Delta S^0/R$.

$$\Delta G^0 = \Delta H^0 - T\Delta S^0 \quad \textbf{(Eq. 14)}$$

$$\Delta G^0 = -RT\ln K_c \quad \textbf{(Eq. 15)}$$

$$K_c = \frac{q_e}{C_e} \quad \textbf{(Eq. 16)}$$

$$\ln K_c = \frac{\Delta S^0}{R} - \frac{\Delta H^0}{RT} \quad \textbf{(Eq. 17)}$$

Hence, in order to evaluate physicochemical characteristics and thermochemical features of Cs adsorption onto vermiculite, thermodynamic studies were conducted. In this context, K_c (q_e/C_e) values for different temperatures (25, 40, 50 and 70 °C) were calculated and different ΔG^0 values for these temperatures were obtained. To calculate ΔH^0 and ΔS^0 values, a graphic of $\ln K_c$ versus 1/T was plotted (Van't Hoff plot) and was displayed in Fig 16. Thermodynamic parameters of adsorption process are given below. Effect of temperature on Cs adsorption is shown in Figure 15, which shows that Cs^+ sorption capacity was decreased with increasing temperatures. Zheng *et al.* (63) observed the same situation, since the temperature increased, Cs uptake on

unmodified montmorillonite diminished. Also, Kim *et al.* (2) reported that Cs sorption gradually decreased with higher temperatures using raw sericite mineral.

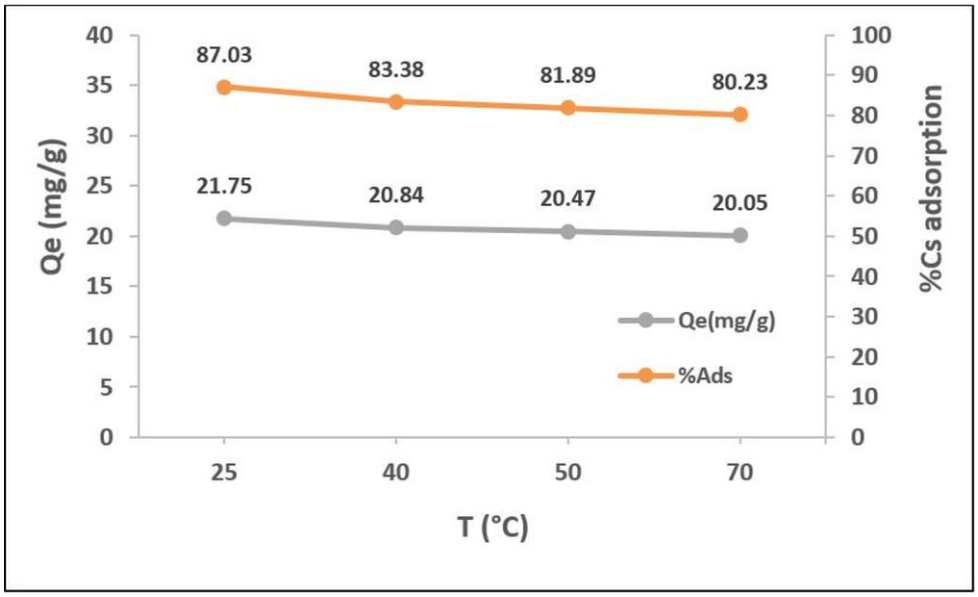

Figure 15: Effect of temperature (Adsorbent dosage: 0.2 g; Initial Cs concentration: 200 mg/L; Volume: 25 mL; Solution pH: 8; Contact time: 5 h).

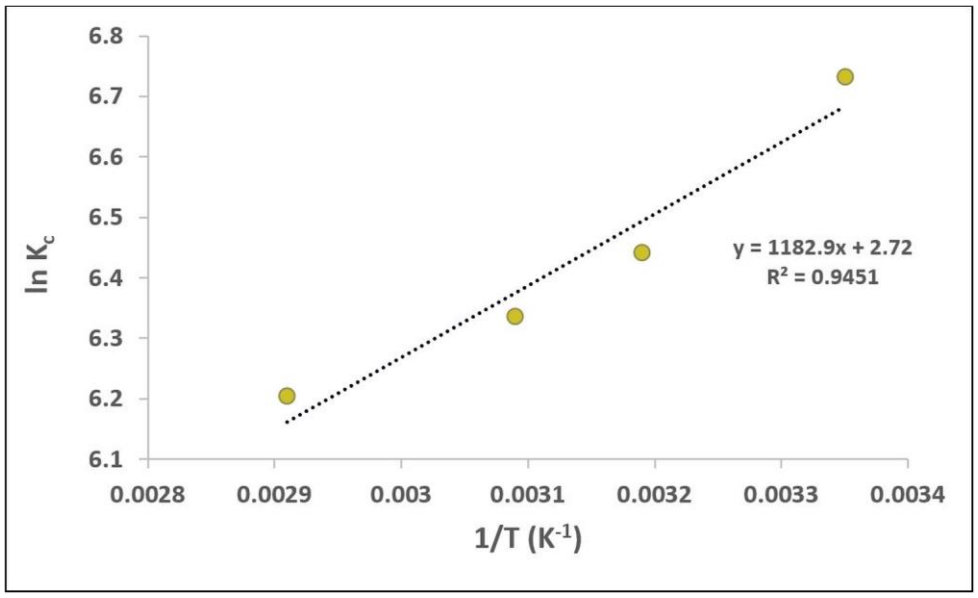

Figure 16: Van't Hoff plot of Cs adsorption.

Results demonstrated that cesium adsorption process onto vermiculite mineral occurred spontaneously, since ΔG^0 values were obtained below zero (-15.65, -16.67, -16.76, -17.02 and -17.69 kJ/mol for 25, 40, 50 and 70 °C, respectively) and higher ΔG^0 values with increasing temperatures revealed that spontaneity increased with increasing temperatures.

The negative ΔH^0 value indicated that sorption of Cs^+ ions on the mineral surface had exothermic character, meaning as the temperature increased, the amount of adsorbed Cs^+ ions were gradually decreased as seen in Figures 24 and 25. Positive ΔS^0 value of 22.61 j/mol.K proved

that the disorderliness among the solid and liquid phases in bulk solution increased during adsorption equilibrium.

The degree of ΔH^0 value provides the knowledge of sorption characteristics, if ΔH^0 value is between 8-25 kJ/mol, the adsorption process is a physisorption and if it is between 83-830 kJ/mol, it is a chemisorption (56). Thus, ΔH^0 value of -9.83 kJ/mol being lower than 25 kJ/mol revealed that Cs adsorption was a physical process with weak interactions between adsorbent and adsorbate molecules. K_c values were decreased with increasing temperatures and that means the mobility of Cs^+ ions were increased with gradual increase in adsorption temperature, referring that interactions between adsorbent and adsorbate molecules were weakened and amount of adsorbed Cs^+ ions were decreased (62).

Results of our study are compared and interpreted with similar studies in literature and given in Table 2.

Table 2. Comparison of current experimental Cs^+ adsorption capacities on different adsorbents.

Adsorbent	**Q_{max}** (mg/g)	**Reference**
Sivas vermiculite (Turkey)	29.67	This study
Gangneung Sericite (Korea)	6.68	(2)
Vermiculite (Commercial)	56.92	(3)
Vermiculite (Natural)	0.65	(4)
Nitric acid-modified bamboo charcoal	45.87	(32)
Potassium cobalt hexacyanoferrate modified leather scrap	36.75	(33)
Nickel modified Akadama clay (Japan)	16.10	(43)
Silica gel embedded phosphotungstic acid	20.80	(44)
Ammonium-pillared montmorillonite/Fe_3O_4	27.53	(63)
Clay from Inshas disposal site, Cairo (Egypt)	46.30	(64)
Nanocrystalline mordenite	37.30	(65)
Chitosan impregnated with ionic liquid	2.85	(66)
Marble	2.37	(67)
Modified hydroxyl apatite	69.49	(68)

These results suggest that vermiculite is a strong and efficient sorbent for Cs^+ removal compared with other clay minerals and various kinds of modified adsorbents. As seen in Table 4, Q_{max} values of some modified adsorbents (nanocrystalline mordenite, nitric acid modified bamboo charcoal, KCoHF modified leather scrap, modified hydroxyl apatite) were higher than that of the present study. However, studied vermiculite is a natural material and this adsorbent can be easily applied with cheap, economic and simple batch sorption procedures in solutions such as water with neutral/low alkaline pH values for Cs removal.

Cesium desorption studies

Recovering adsorbates with nuclear character are crucial in preventing radioactive contamination trapped in soil minerals, which are exposed to the natural environment, and living metabolisms. Hence, Cs^+ ions were desorbed from adsorbent using different kinds of eluent solutions with various concentrations. Results of desorption study were demonstrated in Figure 17 and Table 3, respectively.

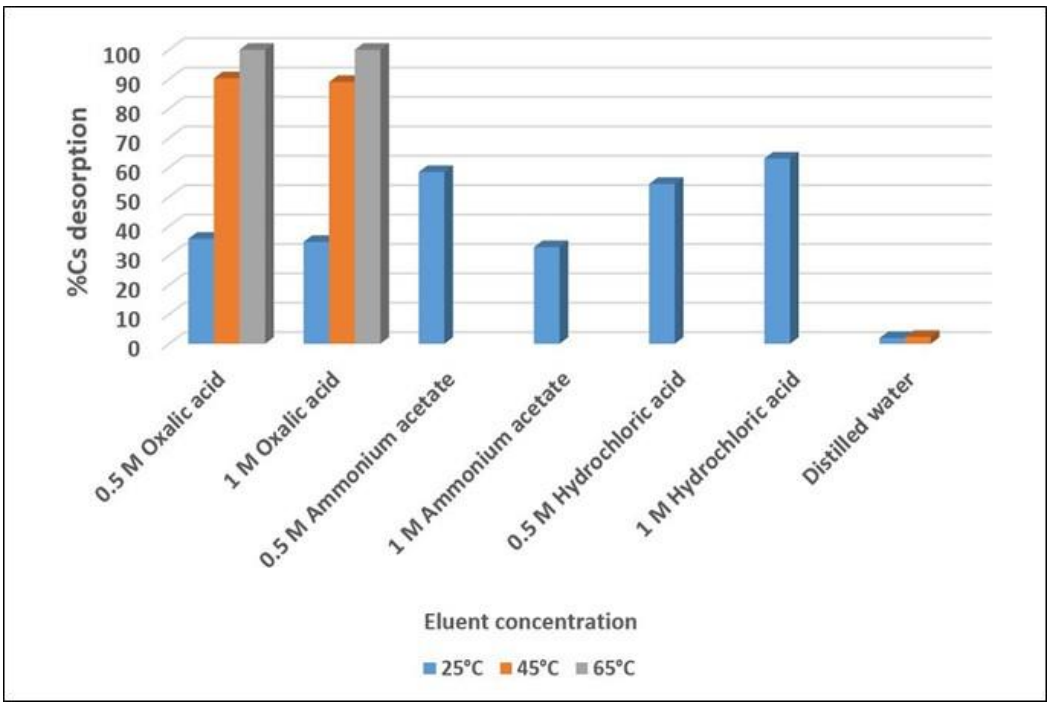

Figure 17: Cs^+ desorption efficiency against eluent concentration.

Results proved that the most efficient recovery of Cs^+ ions from vermiculite surface to solution media occurred using oxalic acid eluent with 89%, 90% and 100% desorption efficiency under 45 and 65 °C (Table 3). The concentration of oxalic acid did not cause a significant difference in desorption efficiency since Cs^+ recovery ratios are nearly the same (Figure 17). 0.5 M ammonium acetate solution caused a stronger regain of Cs^+ than that of 1 M eluent. As for a strong acid HCl, higher concentration provided a slight increase in Cs recovery ratio, as seen in Table 3.

Table 3: Results of Cs desorption studies.

Eluent (volume= 10 mL)	Concentration of eluent (M)	pH	Batch shaker temperature (°C)	Desorption Cs (%)
Oxalic acid	0.5	1.56	25	35.73
Oxalic acid	1	1.48	25	34.65
Oxalic acid	0.5	1.46	45	90.30
Oxalic acid	1	1.48	45	89.06
Oxalic acid	0.5	1.53	65	100
Oxalic acid	1	0.63	65	100
NH_4AOc	0.5	5.72	25	58.44
NH_4AOc	1	6.01	25	32.89
HCl	0.5	0.36	25	54.38
HCl	1	0.23	25	63
Distilled water	-	7.13	25	1.96
Distilled water	-	6.93	45	2.36

Desorption and regeneration of Cs in water are necessary because the most of radioactive Cs^+ exist in aqueous media after nuclear accidents and fallouts. Small amounts of Cs^+ ions were desorbed from adsorbent to water and this indicated that vermiculite trapped Cs into its porous structure strongly, even at higher temperatures than ambient room temperature (45 °C). These results clearly suggest that whether radioactive Cs^+ is adsorbed by vermiculite in water media, it does not tend to be transferred to the liquid phase, preventing the radioactive damage to aqueous media and living organisms.

Potassium interference effect studies

Results of ion interference study were illustrated in Table 4. When the cesium ion concentration (200 mg/L) is two times higher then the potassium concentration (100 mg/L), Cs adsorption yield was found as 64% and the amount of Cs adsorbed at equilibrium was calculated as 16.22 mg/g. It is still a good uptake in the presence of K^+ ions.

Table 4: Results of potassium interference effect study
(vermiculite= 0.2 g, V= 25 mL, pH=8, Contact time= 4 h., Cs conc.= 200 mg/L, temp.=25 °C)

K conc. (mg/L) in solution	Cs, C_e (mg/L)	Cs, q_e (mg/g)	K, C_e (mg/L)	K, q_e (mg/g)	Adsorption Cs (%)	Adsorption K (%)
100	70.28	16.22	106.30	none	64.86	none
400	119	10.12	289	13.88	40.50	27.75

K^+ concentration in seawater was given around 9700 µmol/L (approx. 400 mg/L) for normal salinity. As for low solute fresh waters and rivers, it was in the range of 1-50 µmol/L (approx. 0.04-1.95 mg/L) (69). As seen in Table 4, at 400 ppm of K concentration, Cs adsorption yield was found as 40.50%. For seawater with normal salinity, Cs adsorption yield is acceptable considering the strong constraining effect of K^+ ions due to similar ionic radius with Cs^+ [RK^+=1.33 A° (33), RCs^+=1.70 A° (70)].

CONCLUSIONS

In the current study, Cs removal performance of raw vermiculite obtained from Sivas-Yıldızeli region of Turkey was investigated and 87% of Cs^+ ions were adsorbed under optimal conditions. Adsorption process followed pseudo-second order kinetics model with an excellent R^2 value of 0.9987. Equilibrium studies revealed that Cs adsorption onto vermiculite layer was compatible with Langmuir, Freundlich, and Temkin isotherm models suggesting that Cs uptake on the mineral surface had both physical and chemical sorption character. The maximum adsorption capacity of natural vermiculite (5 h) calculated from the Langmuir model was 29.67 mg/g at 298 K. The adsorption energy value was calculated as 0.772 kJ/mol using D-R isotherm model, being lower than 8 kJ/mol, clearly indicated that the physisorption process was in effect during Cs uptake.

Negative Gibbs energy values obtained with thermodynamic studies showed that adsorption process was spontaneous and had high feasibility, indicating that sorption of Cs^+ ions onto vermiculite surface has not needed an extra external energy to realize. Negative and low enthalpy value indicated that sorption was physicochemically exothermic and interactions between adsorbent and adsorbate ions were weak since the percentage of Cs ions adsorbed at equilibrium decreased with increasing temperatures. Consequently, the positive mid-range value of entropy proposed that disorderliness between the solid and liquid phases in the bulk media increased during adsorption.

Desorption studies showed that oxalic acid was the most efficient elution agent since 100% of Cs was completely recovered from solution media. Potassium interference studies revealed that when the concentration of cesium cation was two times higher than potassium (200 mg/L Cs + 100 mg/L K) during the adsorption, approximately 65% of Cs^+ ions were adsorbed and the value is acceptable. When the concentration of K^+ ions was two times higher than Cs^+ ions in solution media (200 mg/L Cs + 400 mg/L K) which included nearly the same potassium content with natural seawater, 40% of Cs was adsorbed. This is a quite satisfactory yield considering the powerful interfering effect of potassium ions. As a consequence, cesium adsorption is decreased with increasing K^+ concentrations in solution media.

In conclusion, results gathered in present study is a clear demonstration that vermiculite obtained from Sivas-Yıldızeli-Türkiye has an exceptional potential for removing Cs from aqueous media. It indicates that vermiculite mined with national mining procedures could also be used in any nuclear accident for the purpose of decomposing and removing radioactive ^{137}Cs leaked into water media. This, of course, is expected to contribute to national scientific prestige and national economy, whether efficient removal of ^{137}Cs can also be materialized in light of present results since stable ^{133}Cs has same radiochemical features with radioactive ^{137}Cs. Finally, it is expected that the adsorption capacity and Cs^+ ion selectivity of raw vermiculite obtained from Sivas-Karakoç mine can be enhanced with chemical modification using various molecules and better results can be taken with modification in future studies.

ACKNOWLEDGMENTS

Authors thank General Directorate of Mineral Research and Exploration Foundation for their contribution in XRF analysis of vermiculite.

REFERENCES

1. Suzuki N, Ochi K, Chikuma T. Cesium Adsorption Behavior of Vermiculite and It's Application to the Column Method. J Ion Exch. 2014;25(4):122–5.

2. Kim J-O, Lee S-M, Jeon C. Adsorption characteristics of sericite for cesium ions from an aqueous solution. Chem Eng Res Des. 2014 Feb;92(2):368–74.

3. Long H, Wu P, Yang L, Huang Z, Zhu N, Hu Z. Efficient removal of cesium from aqueous solution with vermiculite of enhanced adsorption property through surface modification by ethylamine. J Colloid Interface Sci. 2014 Aug;428:295–301.

4. Hadadi N, Kananpanah S, Abolghasemi H. Equilibrium and Thermodynamic Studies of Cesium Adsorption on Natural Vermiculite and Optimization of Operation Conditions. Iran J Chem Chem Eng IJCCE. 2009 Dec 1;28(4):29–36.

5. Sangvanich T, Sukwarotwat V, Wiacek RJ, Grudzien RM, Fryxell GE, Addleman RS, et al. Selective capture of cesium and thallium from natural waters and simulated wastes with copper ferrocyanide functionalized mesoporous silica. J Hazard Mater. 2010 Oct;182(1–3):225–31.

6. Igwe JC, Abia AA. A bioseparation process for removing heavy metals from waste water using biosorbents. Afr J Biotechnol [Internet]. 2006 Jan 1 [cited 2017 Jun 18];5(11). Available from: https://www.ajol.info/index.php/ajb/article/view/43005

7. Abdel-Ghani NT, Hefny M, El-Chaghaby GAF. Removal of lead from aqueous solution using low cost abundantly available adsorbents. Int J Environ Sci Technol. 2007 Dec;4(1):67–73.

8. Gupta VK, Carrott PJM, Ribeiro Carrott MML, Suhas. Low-Cost Adsorbents: Growing Approach to Wastewater Treatment—a Review. Crit Rev Environ Sci Technol. 2009 Oct 9;39(10):783–842.

9. Kim E-J, Lee C-S, Chang Y-Y, Chang Y-S. Hierarchically Structured Manganese Oxide-Coated Magnetic Nanocomposites for the Efficient Removal of Heavy Metal Ions from Aqueous Systems. ACS Appl Mater Interfaces. 2013 Oct 9;5(19):9628–34.

10. Khan NA, Hasan Z, Jhung SH. Adsorptive removal of hazardous materials using metal-organic frameworks (MOFs): A review. J Hazard Mater. 2013 Jan;244–245:444–56.

11. Uddin MK. A review on the adsorption of heavy metals by clay minerals, with special focus on the past decade. Chem Eng J. 2017 Jan;308:438–62.

12. A. Saleh T, Sarı A, Tuzen M. Chitosan-modified vermiculite for As(III) adsorption from aqueous solution: Equilibrium, thermodynamic and kinetic studies. J Mol Liq. 2016 Jul;219:937–45.

13. Stawinski W, Wegrzyn A, Danko T, Freitas O, Figueiredo S, Chmielarz L. Acid-base treated vermiculite as high performance adsorbent: Insights into the mechanism of cationic dyes adsorption, regeneration, recyclability and stability studies. Chemosphere. 2017 Apr;173:107–15.

14. Gharin Nashtifan S, Azadmehr A, Maghsoudi A. Comparative and competitive adsorptive removal of Ni2+ and Cu2+ from aqueous solution using iron oxide-vermiculite composite. Appl Clay Sci. 2017 May;140:38–49.

15. Malandrino M, Abollino O, Giacomino A, Aceto M, Mentasti E. Adsorption of heavy metals on vermiculite: Influence of pH and organic ligands. J Colloid Interface Sci. 2006 Jul;299(2):537–46.

16. Sawhney BL. Sorption and Fixation of Microquantities of Cesium by Clay Minerals: Effect of Saturating Cations. Soil Sci Soc Am J. 1964;28(2):183.

17. Sawhney BL. Sorption of Cesium from Dilute Solutions. Soil Sci Soc Am J. 1965;29(1):25.

18. Sawhney BL. Unusual Sorption of Caesium by Vermiculite. Nature. 1966 Aug;211(5051):893–4.

19. Sawhney BL. Selective Sorption and Fixation of Cations by Clay Minerals: A Review. Clays Clay Miner. 1972;20(2):93–100.

20. Sikalidis CA, Misaelides P, Alexiades CA. Caesium selectivity and fixation by vermiculite in the presence of various competing cations. Environ Pollut. 1988;52(1):67–79.

21. Japanese Atomic Energy Agency. Radioactive cesium is adsorbed onto vermiculite and biotite, mechanism of cesium adsorption has been clarified [Internet]. Japanese Atomic Energy Agency Sector of Fukushima Research and Development. 2015 [cited 2015 Jan 26]. Available from: https://fukushima.jaea.go.jp/english/topics/pdf/topics-fukushima058e.pdf

22. Staunton S, Dumat C, Zsolnay A. Possible role of organic matter in radiocaesium adsorption in soils. J Environ Radioact. 2002 Jan;58(2–3):163–73.

23. Faithfull NT, editor. Methods in agricultural chemical analysis: a practical handbook [Internet]. Wallingford: CABI; 2002 [cited 2017 Jun 18]. Available from: http://www.cabi.org/cabebooks/ebook/20023165853

24. Santos SSG, Pereira MBB, Almeida RKS, Souza AG, Fonseca MG, Jaber M. Silylation of leached-vermiculites following reaction with imidazole and copper sorption behavior. J Hazard Mater. 2016 Apr;306:406–18.

25. Dias NC, Steiner PA, Braga MCB. Characterization and Modification of a Clay Mineral Used in Adsorption Tests. J Miner Mater Charact Eng. 2015;03(04):277–88.

26. Karakoç Cevherinin Fiziksel ve Kimyasal Özellikleri : Organik Madencilik [Internet]. [cited 2017 Jun 18]. Available from: http://www.organikmadencilik.com/?p=112

27. Dong Z, Qiu Y, Dai Y, Cao X, Wang L, Wang P, et al. Removal of U(VI) from aqueous media by hydrothermal cross-linking chitosan with phosphate group. J Radioanal Nucl Chem. 2016 Sep;309(3):1217–26.

28. Üçgül E. Sivas-Yıldızeli-Karakoç Flogopit Cevherinin Isısal ve Kimyasal Genleşme Özellikleri [Yüksek Mühendislik Tezi]. Hacettepe Üniversitesi; 1997.

29. Addison J. Sivas-Yıldızeli-Karakoç Detaylı Jeolojik Prospeksiyon Çalışması. 2007.

30. Ehsani İ. Bir Vermikülitin Fiziksel, Kimyasal ve Isıl Özellikleri Üzerine Sülfürik Asit Liçinin Etkileri [Yüksek Lisans Tezi]. [Ankara]: Hacettepe Üniversitesi, Fen Bilimleri Enstitüsü, Maden Mühendisliği Anabilim Dalı; 2015.

31. Yalçın H, Bozkaya Ö, Yeşildağ H. Sivas-Yıldızeli Yöresi Ultramafik Platonik Kayaçlarla İlişkili Flogopit Oluşumlarının Kökeni. Yerbilim Üniversitesi Yerbilim Uygul Ve Araşt Merk Derg [Internet]. 2016 Jun 3 [cited 2017 Jun 18];37(1). Available from: http://dergipark.gov.tr/doi/10.17824/yrb.79284

32. Khandaker S, Kuba T, Kamida S, Uchikawa Y. Adsorption of cesium from aqueous solution by raw and concentrated nitric acid–modified bamboo charcoal. J Environ Chem Eng. 2017 Apr;5(2):1456–64.

33. Yang J, Luo X, Yan T, Lin X. Recovery of cesium from saline lake brine with potassium cobalt hexacyanoferrate-modified chrome-tanned leather scrap adsorbent. Colloids Surf Physicochem Eng Asp. 2018 Jan;537:268–80.

34. Lagergren S. About the Theory of So-Called Adsorption of Soluble Substances. K Sven Vetenskapsakademiens Handl. 1898;24(4):1–39.

35. Ho Y., McKay G. Pseudo-second order model for sorption processes. Process Biochem. 1999 Jul;34(5):451–65.

36. Zeldowitsch J. Über den mechanismus der katalytischen oxydation von CO an MnO2. Acta Physicochem URSS. 1934;1:364–449.

37. Ho Y. Review of second-order models for adsorption systems. J Hazard Mater. 2006 Aug 25;136(3):681–9.

38. Low MJD. Kinetics of Chemisorption of Gases on Solids. Chem Rev. 1960 Jun 1;60(3):267–312.

39. Abdel-Ghani NT, Rawash ESA, El-Chaghaby GA. Equilibrium and kinetic study for the adsorption of p-nitrophenol from wastewater using olive cake based activated carbon. Glob J Environ Sci Manag. 2016 Jan 1;2(1):11–8.

40. Nethaji S, Sivasamy A, Mandal AB. Adsorption isotherms, kinetics and mechanism for the adsorption of cationic and anionic dyes onto carbonaceous particles prepared from Juglans regia shell biomass. Int J Environ Sci Technol. 2013 Mar;10(2):231–42.

41. Chen R, Tanaka H, Kawamoto T, Asai M, Fukushima C, Na H, et al. Selective removal of cesium ions from wastewater using copper hexacyanoferrate nanofilms in an electrochemical system. Electrochimica Acta. 2013 Jan;87:119–25.

42. Sakamoto S, Kawase Y. Adsorption capacities of poly-g-glutamic acid and its sodium salt for cesium removal from radioactive wastewaters. J Environ Radioact. 2016 Dec;165:151–8.

43. Ding D, Lei Z, Yang Y, Zhang Z. Efficiency of transition metal modified akadama clay on cesium removal from aqueous solutions. Chem Eng J. 2014 Jan;236:17–28.

44. Seaton K, Little I, Tate C, Mohseni R, Roginskaya M, Povazhniy V, et al. Adsorption of cesium on silica gel containing embedded phosphotungstic acid. Microporous Mesoporous Mater. 2017 May;244:55–66.

45. Langmuir I. The Adsorption of gases on plane surfaces of glass, mica and platinium. J Am Chem Soc. 1918 Sep;40(9):1361–403.

46. Freundlich H. Über die Absorption in Lösungen. Z Für Phys Chem. 1906;57:385–470.

47. Dubinin MM. The Potential Theory of Adsorption of Gases and Vapors for Adsorbents with Energetically Nonuniform Surfaces. Chem Rev. 1960 Apr 1;60(2):235–41.

48. Temkin M, Pyzhev V. Recent modifications to Langmuir isotherms. Acta Physicochim URSS. 1940;12:217–22.

49. Zacaroni LM, Magriotis ZM, Cardoso M das G, Santiago WD, Mendon?a JG, Vieira SS, et al. Natural clay and commercial activated charcoal: Properties and application for the removal of copper from cacha?a. Food Control. 2015 Jan;47:536–44.

50. Bentahar Y, Hurel C, Draoui K, Khairoun S, Marmier N. Adsorptive properties of Moroccan clays for the removal of arsenic(V) from aqueous solution. Appl Clay Sci. 2016 Jan;119:385–92.

51. Khan TA, Singh VV. Removal of cadmium(II), lead(II), and chromium(VI) ions from aqueous solution using clay. Toxicol Environ Chem. 2010 Sep;92(8):1435–46.

52. Priyantha N, Bandaranayaka A. Interaction of Cr(VI) species with thermally treated brick clay. Environ Sci Pollut Res. 2011 Jan;18(1):75–81.

53. Alemayehu D, Singh S, Tessema D. Assessment of the adsorption capacities of fired clay soils from Jimma (Ethiopia) for the removal of Cr (VI) from aqueous solution. Univ J Env Res Technol. 2012;2:411–20.

54. McKay G, Blair HS, Gardner JR. Adsorption of dyes on chitin. I. Equilibrium studies. J Appl Polym Sci. 1982 Aug;27(8):3043–57.

55. Meroufel B, Benali O, Benyahya M, Benmoussa Y, Zenasni M. Adsorptive removal of anionic dye from aqueous solutions by Algerian kaolin: Characteristics, isotherm, kinetic and thermodynamic studies. J Mater Env Sci. 2013;4(3).

56. Vijayakumar G, Tamilarasan R, Dharmendirakumar M. Adsorption, Kinetic, Equilibrium and Thermodynamic studies on the removal of basic dye Rhodamine-B from aqueous solution by the use of natural adsorbent perlite. J Mater Env Sci. 3(1):157–70.

57. Wibowo E, Rokhmat M, Sutisna, Khairurrijal, Abdullah M. Reduction of seawater salinity by natural zeolite (Clinoptilolite): Adsorption isotherms, thermodynamics and kinetics. Desalination. 2017 May;409:146–56.

58. Kyziol-Komosinska J, Rosik-Dulewska C, Franus M, Antoszczyszyn-Szpicka P, Czupiol J, Krzyzewska I. Sorption Capacities of Natural and Synthetic Zeolites for Cu(II) Ions. Pol J Environ Stud. 2015;24:1111–23.

59. Can N, Ömür BC, Altındal A. Modeling of heavy metal ion adsorption isotherms onto metallophthalocyanine film. Sens Actuators B Chem. 2016 Dec;237:953–61.

60. Hasany SM, Chaudhary MH. Sorption potential of Haro river sand for the removal of antimony from acidic aqueous solution. Appl Radiat Isot. 1996 Apr;47(4):467–71.

61. Ibrahim MB, Sani S. Comparative Isotherms Studies on Adsorptive Removal of Congo Red from Wastewater by Watermelon Rinds and Neem-Tree Leaves. Open J Phys Chem. 2014;04(04):139–46.

62. Lian L, Guo L, Guo C. Adsorption of Congo red from aqueous solutions onto Ca-bentonite. J Hazard Mater. 2009 Jan;161(1):126–31.

63. Zheng X, Dou J, Yuan J, Qin W, Hong X, Ding A. Removal of Cs + from water and soil by ammonium-pillared montmorillonite/Fe3O4 composite. J Environ Sci. 2017 Jun;56:12–24.

64. Abdel-Karim A-AM, Zaki AA, Elwan W, El-Naggar MR, Gouda MM. Experimental and modeling investigations of cesium and strontium adsorption onto clay of radioactive waste disposal. Appl Clay Sci. 2016 Nov;132–133:391–401.

65. Lee K-Y, Park M, Kim J, Oh M, Lee E-H, Kim K-W, et al. Equilibrium, kinetic and thermodynamic study of cesium adsorption onto nanocrystalline mordenite from high-salt solution. Chemosphere. 2016 May;150:765–71.

66. Lupa L, Voda R, Popa A. Adsorption behavior of cesium and strontium onto chitosan impregnated with ionic liquid. Sep Sci Technol. 2017 Apr 10;1–9.

67. Hamed MM, Aly MI, Nayl AA. Kinetics and thermodynamics studies of cobalt, strontium and caesium sorption on marble from aqueous solution. Chem Ecol. 2016 Jan 2;32(1):68–87.

68. Metwally SS, Ahmed IM, Rizk HE. Modification of hydroxyapatite for removal of cesium and strontium ions from aqueous solution. J Alloys Compd. 2017 Jun;709:438–44.

69. Talling JF. Potassium — A Non-Limiting Nutrient in Fresh Waters? Freshw Rev. 2010 Dec;3(2):97–104.

70. Onodera M, Kirishima A, Nagao S, Takamiya K, Ohtsuki T, Akiyama D, et al. Desorption of radioactive cesium by seawater from the suspended particles in river water. Chemosphere. 2017 Oct;185:806–15.